Reduced Basis Model Reduction of Parametrized Two–Phase Flow in Porous Media ⋆

Martin Drohmann * **Bernard Haasdonk** ** **Mario Ohlberger** ***

* *Institute of Numerical and Applied Mathematics, University of Münster, 48149 Münster, Germany (*mdrohmann@uni-muenster.de*)*
** *Institute of Applied Analysis and Numerical Simulation, University of Stuttgart, 70569 Stuttgart, Germany (*haasdonk@math.uni-stuttgart.de*)*
*** *Institute of Numerical and Applied Mathematics, University of Münster, 48149 Münster, Germany (*ohlberger@uni-muenster.de*)*

Abstract: Many applications, e.g. in control theory and optimization depend on time–consuming parameter studies of parametrized evolution equations. Reduced basis methods are an approach to reduce the computation time of numerical simulations for these problems. The methods have gained popularity for model reduction of different numerical schemes with remarkable results preferably for scalar and linear problems with affine dependence on the parameter as in Patera and Rozza (2007). Over the last few years, the framework for the reduced basis methods has been continuously extended for non–linear discretizations, coupled problems and arbitrary dependence on the parameter, e.g. Grepl et al. (2007); Drohmann et al. (2010); Carlberg et al. (2011).
In this presentation, we apply the framework developed in Drohmann et al. (2010) on a problem that combines all these difficulties. The considered problem models two–phase flow in a porous medium discretized by the finite volume method like in Michel (2004). For a first test, we do noth parametrize the problem and concentrate on the development of an efficient reduced basis scheme. This allows for separate approximations of the function spaces for the three physical unknowns and the non–linear terms in this numerical scheme.
We shortly introduce the main aspects of the reduced basis method including the concept of offline/online decomposition, empirical operator interpolation method and reduced basis generation by greedy algorithms. We discuss how the coupling of the unknowns — saturation, velocity and pressure — must be reflected in the generated reduced spaces.

Keywords: Reduced basis method, two–phase flow, finite volume method, empirical operator interpolation, proper orthogonal decomposition

1. INTRODUCTION

Reduced basis (RB) methods are popular methods for model order reduction of problems with parametrized partial differential equations that need to be solved for many parameters. Such scenarios might occur in parameter studies, optimization, control, inverse problems or statistical analysis for a given parametrized problem. The introduction of the parametrization into the model allows for construction of low–dimensional function spaces — the so–called RB spaces — which approximate the set of all admissible solutions. Developing a reduced scheme by a Galerkin projection onto this space leads to efficient and reliable reduced simulations. The construction of the RB space involves high–dimensional computations and thus needs high computational resources. This gives rise to the concept of *offline/online decomposition* separating the high–dimensional computations (including the basis generation) in the *offline* phase from the *online* phase with efficient reduced simulations for many parameters.

The method has been applied on different problem classes with stationary, linear problems with affine dependence on the parameter on the one end (e.g. Patera and Rozza (2007); Haasdonk and Ohlberger (2008)) and lately also to non–linear, non–stationary systems of partial differential equations on the other end (c.f. Carlberg et al. (2011), Chaturantabut and Sorensen (2011)). In this presentation, we also deal with the latter problem class, handling the model reduction of the function spaces for all physical unknowns separately. We apply the empirical interpolation and the reduced basis framework as developed in Drohmann et al. (2010) to a system of two non–linear coupled partial differential equations modelling two-phase flow in porous media:

⋆ This work was supported by German Science Foundation (DFG) under the contract number OH 98/2-1. The second author was supported by the Baden-Wrttemberg Stiftung gGmbH and thanks the German Science Foundation (DFG) for financial support within the Cluster Of Excellence in Simulation Technology (EXC 310/1) at the University of Stuttgart.

$$\partial_t s + \nabla \cdot (f(s)\mathbf{u} - v(s)\nabla s) = q_1 \quad \text{in } \Omega \times [0,T], \tag{1}$$
$$\nabla \cdot (M(s)\nabla \psi) = q_1 + q_2 \quad \text{in } \Omega \times [0,T], \tag{2}$$
$$(\mathbf{u} = -M(s)\nabla \psi) \quad \text{in } \Omega \times [0,T] \tag{3}$$

The problem is situated on a bounded domain $\Omega \subset \mathbb{R}^2$ modelling a porous medium, and is given in the so-called global pressure formulation with unknowns s for the saturation of the wetting phase, the global pressure ψ and the total velocity flow $\mathbf{u}$. The global pressure ψ is an artificial magnitude which is derived from the pressure p of the wetting fluid and the empirically known capillary pressure curve p_c via

$$\psi = p + \int_0^s f(x) p_c'(x) \mathrm{d}x. \tag{4}$$

The model functions $f, M, p_c : [0,1] \to \mathbb{R}$ characterize the the fractional flow rate, the mobility rate and the capillary pressure curve. The last one is closely related to the diffusion function $v : [0,1] \to \mathbb{R}, s \mapsto k_w(s) f(s) p_c(s)$, where k_w is the relative permeability of the wetting phase. Furthermore, the source terms are assumed to be of the form

$$q_1(s) = c\overline{q} - s\underline{q} \qquad \text{and} \qquad q_2(s) = (1-c)\overline{q} - (1-s)\underline{q} \tag{5}$$

modelling injection or production wells, where $c \in [0,1]$ is an injection constant.

In order to close the system (1-3), we introduce Neumann boundary conditions $\nabla s \cdot \mathbf{n} = 0$ and $\nabla \psi \cdot \mathbf{n} = 0$ on $\partial\Omega \times [0,T]$, prescribe an initial saturation $s(\cdot, 0) = s_0$ and define the global pressure to have zero mean

$$\int_\Omega \psi(x, \cdot) \mathrm{d}x = 0 \quad \text{in } \Omega \times [0,T], \tag{6}$$

as it is defined up to a constant only, otherwise. For the first test of a reduced scheme presented in this work, we refrain from a parametrization of the problem.

For details on the derivation of the global pressure formulation of two–phase flow problems, we refer to Michel (2004), which also serves as source for the discretization of the above equations and the model data used in our numerical computations. This fully implicit finite volume scheme is summarized in the next section. We identified two non–linear operators in the scheme and show in Section 3 how they are empirically interpolated. In Section 4 the reduced scheme derived by a Galerkin projection onto the reduced basis scheme and the offline/online decomposition of this scheme is described. We conclude this proceedings article with experiments and a discussion on the separate reduction of the three physical magnitudes.

2. FINITE VOLUME DISCRETIZATION

In this section, we summarize the fully implicit finite volume scheme from Michel (2004) reformulated in a notation suitable for the model reduction in the following sections. First, we introduce an admissible mesh on Ω consisting of a set of convex control volumes $\mathcal{T} := \{e_i\}_{i=1}^H$, a family of edges $\mathcal{E}$ with $\sigma \subset \bar{\Omega}$ for all $\sigma \in \mathcal{E}$ and a family of control volume centers $\{x_i\}_{i=1}^H$ with $x_i \in e_i$ for $i = 1, \dots, H$. Further properties of the mesh are:

(1) $\cup_{i=1}^H \overline{e_i} = \bar{\Omega}$,

(2) For any $e, f \in \mathcal{T}$ with $e \neq f$, either $m(\bar{e} \cap \bar{f}) = 0$ or $\bar{e} \cap \bar{f} = \bar{\sigma}$ for a $\sigma \in \mathcal{E}$. The set of neighbouring control volumes is denoted by $\mathcal{N}(e) := \{f \in \mathcal{T} |\, m(\bar{e} \cap \bar{f}) \neq 0\}$.

(3) For any cell $e \in \mathcal{T}$ its boundary is given by a set of edges $\mathcal{E}(e) \subset \mathcal{E}$, i.e. $\partial e = \cup_{\sigma \in \mathcal{E}(e)} \bar{\sigma}$.

(4) The connection of two points x_i, x_j is orthogonal to the edge $\sigma_{ij} := \bar{e}_i \cap \bar{e}_j$ and its length is denoted by $d_{ij} := |x_i - x_j|$.

Given an admissible mesh on Ω, we define the two Hilbert spaces $\mathcal{W}_h^\mathcal{T}$ and $\mathcal{W}_h^\mathcal{E}$. These spaces comprise functions $f : \Omega \to \mathbb{R}$ and $f : \mathcal{S} \to \mathbb{R}$ which are piecewise constant on grid control volumes and edges of the mesh, respectively. Here, $\mathcal{S} := \cup_{\sigma \in \mathcal{E}} \bar{\sigma}$ denotes the mesh skeleton. The spaces are equipped with the scalar products $\langle u_h, v_h \rangle_{\mathcal{W}_h^\mathcal{T}} := \int_\Omega u_h v_h$ and $\langle u_h, v_h \rangle_{\mathcal{W}_h^\mathcal{E}} := \int_\mathcal{S} u_h v_h$. As the discrete functions are piecewise constant, they can be identified by vectors of degrees of freedom $(s_{h,i})_{i=1}^H$ and $(u_{h,\sigma})_{\sigma \in \mathcal{E}}$ for functions $s_h \in \mathcal{W}_h^\mathcal{T}$ and $u_h \in \mathcal{W}_h^\mathcal{E}$, respectively. Furthermore, we define the projection operator $\mathcal{P}_h^\mathcal{T} : L^2(\Omega) \to \mathcal{W}_h^\mathcal{T}$ by $\left(\mathcal{P}_h^\mathcal{T}[u]\right)_i := \frac{1}{m(e_i)} \int_{e_i} u$ with $m(e_i)$ being the measure of a control volume e_i for $i = 1, \dots, H$.

We define two non-linear operators $\mathcal{L}_h^s : \mathcal{W}_h^\mathcal{T} \times \mathcal{W}_h^\mathcal{E} \to \mathcal{W}_h^\mathcal{T}$, $\mathcal{L}_h^\mathbf{u} : \mathcal{W}_h^\mathcal{T} \times \mathcal{W}_h^\mathcal{T} \to \mathcal{W}_h^\mathcal{E}$ and one linear operator $\mathcal{L}_h^\psi : \mathcal{W}_h^\mathcal{E} \to \mathcal{W}_h^\mathcal{T}$ discretizing the equations (1)-(3). The saturation operator is given by

$$\begin{aligned}\left(\mathcal{L}_h^s[s_h, \mathbf{u}_h]\right)_i = &\sum_{\sigma \in \mathcal{E}(e_i)} g_\sigma(\mathbf{u}_h, s_h) \\ &- \sum_{e_j \in \mathcal{N}(e_i)} \{v(s_h)\}_{ij} \frac{m(\sigma_{ij})}{d_{ij}} (s_{h,j} - s_{h,i})\end{aligned} \tag{7}$$

where $\{\cdot\}_{ij}$ is the harmonic mean on the edge σ_{ij} and $g_\sigma : \mathcal{W}_h^\mathcal{E} \times \mathcal{W}_h^\mathcal{T} \to \mathbb{R}$ is an upwind finite volume flux

$$g_{\sigma_{ij}}(\mathbf{u}_h, s_h) := \begin{cases} \mathbf{u}_{h,\sigma_{ij}} f(s_{h,i}) & \text{if } \mathbf{u}_{h,\sigma_{ij}} > 0 \\ \mathbf{u}_{h,\sigma_{ij}} f(s_{h,j}) & \text{if } \mathbf{u}_{h,\sigma_{ij}} \leq 0. \end{cases} \tag{8}$$

The velocity operator is defined by

$$\left(\mathcal{L}_h^\mathbf{u}[s_h, \psi_h]\right)_{\sigma_{ij}} = \{M(s_h)\}_{\sigma_{ij}} \frac{m(\sigma_{ij})}{d_{ij}} (\psi_{h,j} - \psi_{h,i}) \tag{9}$$

and the pressure operator by

$$\left(\mathcal{L}_h^\psi[\mathbf{u}_h]\right)_i = \sum_{\sigma \in \mathcal{E}(e_i)} \mathbf{u}_{h,\sigma}. \tag{10}$$

Definition 2.1. (High-dimensional scheme). Given a discretization of the time interval $[0,T]$ by a sequence of $K+1$ strictly increasing time instances $t^k := k\Delta t$, $k = 0, \cdots, K$ with a global time step size $\Delta t > 0$, we are searching for discrete solutions $u_h^k := (s_h^k, \mathbf{u}_h^k, \psi_h^k) \in \mathcal{W}_h := \mathcal{W}_h^\mathcal{T} \times \mathcal{W}_h^\mathcal{E} \times \mathcal{W}_h^\mathcal{T}$. These are computed by an initial projection

$$\left(s_h^0, \mathbf{u}_h^0, \psi_h^0\right) = \left(\mathcal{P}_h^\mathcal{T}[s_0], 0, 0\right) \tag{11}$$

and subsequently solving the equation

$$\mathcal{L}_h\left[s_h^{k+1}, \mathbf{u}_h^{k+1}, \psi_h^{k+1}\right] = 0 \tag{12}$$

with the Newton–Raphson method. In each Newton step, we solve for the defect $\delta^{k+1,\nu+1}$ in

$$\mathbf{D}\mathcal{L}_h|_{u_h^{k+1,\nu}}\left[\delta^{k+1,\nu+1}\right] = -\mathcal{L}_h\left[u_h^{k+1,\nu}\right], \tag{13}$$

where $u_h^{k+1,0} := u^k$ and $u_h^{k+1,\nu+1} := u_h^{k+1,\nu} + \delta^{k+1,\nu+1}$ define the updates in each newton step, and the solution at

each time instance t^k is given by $u_h^{k+1} := u_h^{k+1,\nu_{\max}(k)}$. The last Newton step index $\nu_{\max}^k$ equals the smallest integer ν satisfying $\left\| \mathcal{L}_h \left[u_h^{k+1,\nu+1} \right] \right\| \leq \varepsilon^{\text{New}}$.

Here, $\mathcal{L}_h[s_h^{k+1}, \mathbf{u}_h^{k+1}, \psi_h^{k+1}]$ evaluates to

$$\begin{pmatrix} \frac{1}{\Delta t}\left(s_h^{k+1} - s_h^k\right) - \mathcal{L}_h^s\left[s_h^{k+1}, \mathbf{u}_h^{k+1}\right] - \mathcal{P}_h^{\mathcal{T}}[q_1] \\ \mathcal{L}_h^{\mathbf{u}}[s_h^{k+1}, \psi_h^{k+1}] - \mathbf{u}_h^{k+1} \\ \mathcal{L}_h^{\psi}[u_h^{k+1}] - \mathcal{P}_h^{\mathcal{T}}[q_1 + q_2] \\ \int_\Omega p_h^{k+1} \end{pmatrix}, \quad (14)$$

with the row entries corresponding to the discretizations of equations (1)-(3) and (6).

3. EMPIRICAL OPERATOR INTERPOLATION

For efficient reduced simulations of the above described numerical scheme, we want to substitute the non–linear operators $\mathcal{L}_h^s$ and $\mathcal{L}_h^{\mathbf{u}}$ by efficiently computable surrogates. These so-called empirical operator interpolants will depend on exact operator evaluations in a few interpolation points from which a global result is interpolated in a linear function space.

This idea was originally proposed by Barrault et al. (2004) for discrete functions and extended for general discrete operators in Haasdonk et al. (2007) and Drohmann et al. (2010). In this section, we want to summarize the procedure of the latter paper for an arbitrary and parametrized operator $\mathcal{L}_h(\boldsymbol{\mu}) : \widehat{\mathcal{W}} \to \mathcal{W}$ with a parameter $\boldsymbol{\mu}$ from a finite dimensional set of parameter vectors $\mathcal{M} \subset \mathbb{R}^p$. Here, $\widehat{\mathcal{W}}, \mathcal{W}$ are finite dimensional function spaces. The spaces $\widehat{\mathcal{W}}, \mathcal{W}$ also need to be equipped with a finite element basis as defined in Ciarlet (1978). That is, they come with a set $\Sigma_h := \{\tau_i\}_{i=1}^H$ of linearly independent functionals, which are unisolvent, i.e. there exist unique functions $\psi_i \in \mathcal{W}, i = 1, \ldots, H$ satisfying

$$\tau_j(\psi_i) = \delta_{ij}, \quad 1 \leq j \leq H.$$

The linear functionals $\tau_i, i = 1, \ldots, H$ are called the *degrees of freedom* (DOFs) of the discrete function space $\mathcal{W}$ and the functions $\psi_i, i = 1, \ldots, H$ are called *basis functions*. Note, that the finite volume space $\mathcal{W}_h^{\mathcal{T}}$ and also the function space $\mathcal{W}_h^{\mathcal{E}}$ both have such a Ciarlet basis, where the DOFs are given by evaluations in the control volume centers or the edge midpoints, respectively.

Now, the empirical operator interpolation method can briefly be expressed based on a set of interpolation DOFs $\Sigma_M := \{\tau_m^{EI}\}_{m=1}^M \subset \Sigma_h$ and a corresponding interpolation basis $\boldsymbol{\xi}_M := \{\xi_m\}_{m=1}^M \subset \mathcal{W}$ with $\tau_{m'}^{EI}[\xi_m] = \delta_{m,m'}$ for $1 \leq m, m' \leq M$. Assuming the existence of these sets, the discrete operators can be approximated by an empirical interpolant $\mathcal{I}_M[\mathcal{L}_h(\boldsymbol{\mu})]$ of the form

$$\mathcal{I}_M\left[\mathcal{L}_h(\boldsymbol{\mu})\right][v_h] := \sum_{m=1}^M \tau_m^{\text{EI}}\left(\mathcal{L}_h(\boldsymbol{\mu})[v_h]\right)\xi_m \approx \mathcal{L}_h(\boldsymbol{\mu})[v_h] \quad (15)$$

for all $v_h \in \widehat{\mathcal{W}}$. The sum is assumed to contain few terms, i.e. $M \ll H$.

Algorithm 1 Greedy algorithm for EI basis generation

EI-GREEDY($\mathcal{M}_{\text{train}}, \varepsilon_{\text{tol}}, M_{\max}$)
  $M \leftarrow M_0$
repeat
  for all $(u_h, \boldsymbol{\mu}) \in \mathcal{M}_{\text{train}}$ **do**
    – *Compute exact operator evaluation*
      $v_h \leftarrow \mathcal{L}_h(\boldsymbol{\mu})[u_h]$
      on an argument u_h.
    – *Compute interpolation coefficients*
      $\boldsymbol{\sigma}^M(u_h) := \left(\sigma_j^M(u_h)\right)_{j=1}^M \in \mathbb{R}^M$
      by solving the linear equation system
      $$\sum_{j=1}^M \sigma_j^M(u_h)\tau_i^{EI}[q_j] = \tau_i^{EI}[v_h], \quad (16)$$
      for $i = 1, \ldots, M$
    – *Compute the residual between* v_h *and its current interpolant.*
      $r_M(u_h) \leftarrow v_h - \sum_{j=1}^M \sigma_j^M(u_h) q_j$
  end for
  – *Find operator evaluation* v_h *maximizing* $\|r_M(u_h)\|_{\mathcal{W}}$ over $(u_h, \boldsymbol{\mu}) \in \mathcal{M}_{\text{train}}$.
  – *Find interpolation DOF maximizing the residual.*
    $\tau_{M+1}^{EI} \leftarrow \arg\sup_{\tau \in \Sigma_h} |\tau(r_M(\boldsymbol{\mu}))|$
  – *Normalize to obtain a new basis function.*
    $q_{M+1} \leftarrow (\tau_{M+1}^{EI}(r_M))^{-1} \cdot r_M$
    $M \leftarrow M + 1$
until $\max_{\boldsymbol{\mu} \in \mathcal{M}_{\text{train}}} \|r_M(\boldsymbol{\mu})\|_{\mathcal{W}} \leq \varepsilon_{\text{tol}}$ *or* $M > M_{\max}$
return *collateral reduced basis:* $(\mathbf{Q}_M, \Sigma_h)$

An efficient evaluation of the functionals $\tau_m^{EI}\left(\mathcal{L}_h(\boldsymbol{\mu})[v_h]\right)$ requires it to depend on few basis functions only. This fact inspires the following definition.

Definition 3.1. (H-independent DOF dependence). A discrete operator $\mathcal{L}_h(\boldsymbol{\mu}) : \widehat{\mathcal{W}} \to \mathcal{W}$ fulfills an *H-independent DOF dependence*, if there exists a constant $C \ll H$ independent of H such that for all $\tau \in \Sigma_h$ a restriction operator

$$\mathcal{R}_\tau^C : \widehat{\mathcal{W}} \to \widehat{\mathcal{W}}, v_h = \sum_{i=1}^V \hat{\tau}_i(v_h)\hat{\psi}_i \mapsto \sum_{j \in I_\tau} \hat{\tau}_j(v_h)\hat{\psi}_j$$

exists that restricts the operator argument to $|I_\tau| \leq C$ degrees of freedom and the equation

$$\tau\left(\mathcal{L}_h(\boldsymbol{\mu})[v_h]\right) = \tau\left(\mathcal{L}_h(\boldsymbol{\mu})\left[\mathcal{R}_\tau^C[v_h]\right]\right)$$

still holds for all $v_h \in \widehat{\mathcal{W}}$.

Remark 3.2. In particular, finite element or finite volume operators fulfill the H-independent DOF dependence, as a point evaluation of an operator application only requires data of the argument on neighbouring grid cells together with geometric information of this subgrid.

Assuming this H-independence condition for a parametrized discrete operator, its empirical interpolant can be evaluated efficiently, i.e. independent of the dimension H.

3.1 Basis generation

The generation process for the basis functions and interpolations points works similarly to the algorithm described in the original empirical interpolation paper Barrault et al. (2004) in which point evaluations in so-called "magic

points" are used as interpolation DOFs after the basis functions were selected. The main idea is a greedy algorithm which iteratively enhances the reduced space with new basis functions searched from a training set of suitable operator evaluations. The selection of these basis functions is controlled by minimizing the interpolation error over the finite set $\mathcal{M}_{\text{train}}$ comprising tuples of operator arguments and operator parameters. For the empirical interpolation of the saturation operator $\mathcal{L}_h^s$, e.g., the training set comprises the snapshots

$$\left\{ s_h^{k,\nu}, \mathbf{u}_h^{k,\nu} \right\}_{(k,\nu)\in\mathbf{K}}$$

with $\mathbf{K} := \{(k,\nu) \in \{0,\cdots,K\} \times \mathbb{N}_+; \nu \leq \nu_{\max}(k)\}$ denoting the index set of all (intermediate) solution snapshots of the scheme from Definition 2.1. Here, we do not need to attach parameters to the snapshots in the training set, as the operator is not parametrized.

Algorithm 1 describes the basis generation strategy for the empirical interpolation components. Instead of the nodal basis $\boldsymbol{\xi}_M$ introduced above, this algorithm returns an equivalent basis $\mathbf{Q}_M := \{q_m\}_{m=1}^M$ with a different structure, such that $\tau_m^{EI}[q_m] = 1$ and $\tau_{m'}^{EI}[q_m] = 0$ for all $m' > m$. Unlike the nodal basis, $\mathbf{Q}_M$ is constructed iteratively, such that $\mathbf{Q}_{M-1} \subset \mathbf{Q}_M$ and the basis functions' maximum norm is bound by one $\|q_m\|_{L^\infty(\Omega)} \leq 1$. Because of this property, which makes computations numerically more stable, we use the basis $\mathbf{Q}_M$ in our implementations. The nodal basis $\boldsymbol{\xi}_M$, however, is used in this article for a simpler exposition of the empirical interpolation (15). It can be efficiently constructed from $\mathbf{Q}_M$, because of the lower–triangular shape of the column matrix of basis vectors $q_m, m = 1,\ldots,M$.

Remark 3.3. We mention, that the loop over the training set $\mathcal{M}_{\text{train}}$ which is necessary to find the worst approximation parameters in Algorithm 1, can be executed in parallel with hardly any communication costs. Here, only the scalar results of the residual norms need to be communicated, such that the offline computation time can be extremely improved by use of parallel hardware.

3.2 Empirical interpolation of Fréchet derivatives

Many solvers for numerical approximations of nonlinear partial differential equations use the Newton method to resolve the nonlinearities in the equation and therefore depend on derivatives of discrete operators. It is easy to observe that the Fréchet derivative can also be applied to the empirical interpolant of an operator $\mathcal{L}_h(t,\boldsymbol{\mu})$ as

$$\mathbf{D}\left(\mathcal{I}_M\left[\mathcal{L}_h(t,\boldsymbol{\mu})|_{u_h}\right]\right)[\cdot] = \sum_{m=1}^{M} \mathbf{D}\left(\tau_m^{EI} \circ \mathcal{L}_h(t,\boldsymbol{\mu})|_{u_h}\right)[\cdot]\,\xi_m. \quad (17)$$

4. REDUCED BASIS SCHEME

In this section, we want to show how to reduce the Newton scheme defined in Definition 2.1. We need reduced basis spaces $\mathcal{W}_{\text{red}}^{s,p} \subset \mathcal{W}_h^{\mathcal{T}}$ and $\mathcal{W}_{\text{red}}^{\mathbf{u}} \subset \mathcal{W}_h^{\mathcal{E}}$ spanned by reduced bases $\Phi^* := \{\varphi_n^*\}_{n=1}^{N_*}$ with $* = \{s,\mathbf{u},\psi\}$ and empirical interpolation basis spaces $\boldsymbol{\xi}^s := \{\xi_m^s\}_{m=1}^{M_s}$, $\boldsymbol{\xi}^{\mathbf{u}} := \{\xi_m^{\mathbf{u}}\}_{m=1}^{M_{\mathbf{u}}}$ together with interpolation points $T_M^s := \{x_m^s\}_{m=1}^{M_s}$, $T^{\mathbf{u}} := \{x_m^{\mathbf{u}}\}_{m=1}^{M_{\mathbf{u}}}$ for the empirical operator interpolation of the non–linear operators $\mathcal{L}_h^s$ and $\mathcal{L}_h^{\mathbf{u}}$.

The reduced basis spaces can be obtained by a proper orthogonal decomposition of the "snapshots" $s^{k,\nu}, \mathbf{u}^{k,\nu}$ and $\psi^{k,\nu}$ for all $(k,\nu) \in \mathbf{K}$, i.e. of the entire trajectory of solution snapshots and the intermediate solutions generated by the Newton method.

The empirical interpolation data for the two operators is obtained by the EI-GREEDY algorithm as described in Section 3.

The numerical scheme in Definition 2.1 can then be reduced by searching for reduced solutions $u_{\text{red}} := \left(s_{\text{red}}^k, \mathbf{u}_{\text{red}}^k, \psi_{\text{red}}^k\right) \in \mathcal{W}_{\text{red}}$ for which in each time instance the residual of the reduced operator evaluation $\mathcal{L}_{\text{red}}[s_{\text{red}}^{k+1}, \mathbf{u}_{\text{red}}^{k+1}, \psi_{\text{red}}^{k+1}]$ gets minimized. This operator is defined like its high–dimensional counterpart in (14) where the operators $\mathcal{L}_h^{\{s,\mathbf{u},\psi\}}$ are replaced by reduced surrogates defined as

$$\mathcal{L}_{\text{red}}^s := \mathcal{P}_{\text{red}}^s \circ \mathcal{I}_{M^s}\left[\mathcal{L}_h^s\right], \quad (18)$$

$$\mathcal{L}_{\text{red}}^{\mathbf{u}} := \mathcal{P}_{\text{red}}^{\mathbf{u}} \circ \mathcal{I}_{M^{\mathbf{u}}}\left[\mathcal{L}_h^{\mathbf{u}}\right] \text{ and} \quad (19)$$

$$\mathcal{L}_{\text{red}}^{\psi} := \mathcal{P}_{\text{red}}^{\psi} \circ \mathcal{L}_h^{\psi} \quad (20)$$

with orhogonal projection operators $\mathcal{P}_{\text{red}}^s : \mathcal{W}_h^s \to \mathcal{W}_{\text{red}}^s$, $\mathcal{P}_{\text{red}}^{\psi} : \mathcal{W}_h^{\psi} \to \mathcal{W}_{\text{red}}^{\psi}$ and $\mathcal{P}_{\text{red}}^{\mathbf{u}} : \mathcal{W}_h^{\mathbf{u}} \to \mathcal{W}_{\text{red}}^{\mathbf{u}}$.

4.1 Offline/Online decomposition

The reduced basis scheme is decomposable into a an *offline* phase with computations depending on the high dimension of the original function space $\mathcal{W}_h$ and into an *online* phase with memory efficient and fast reduced simulations. In order to make this decomposition clear, we write down the DOF-wise computations needed to evaluate the reduced operator

$$\mathcal{L}_{\text{red}} : \mathcal{W}_{\text{red}}^s \times \mathcal{W}_{\text{red}}^{\mathbf{u}} \times \mathcal{W}_{\text{red}}^{\psi} \to \mathcal{W}_{\text{red}}^s \times \mathcal{W}_{\text{red}}^{\mathbf{u}} \times \mathcal{W}_{\text{red}}^{\psi} \times \mathbb{R}.$$

We introduce the DOF vectors

$$\mathbf{a}^k := \left(a_n^k\right)_{n=1}^{N_s}, \mathbf{b}^k := \left(b_n^k\right)_{n=1}^{N_{\mathbf{u}}} \text{ and } \mathbf{c}^k := \left(c_n^k\right)_{n=1}^{N_{\psi}},$$

such that $s_{\text{red}}^k = \sum_{n=1}^{N_s} a_n^k \varphi_n^s$, $\mathbf{u}_{\text{red}}^k = \sum_{n=1}^{N_{\mathbf{u}}} b_n^k \varphi_n^{\mathbf{u}}$ and $\psi_{\text{red}}^k = \sum_{n=1}^{N_{\psi}} c_n^k \varphi_n^{\psi}$. Then the $n-$th degree of freedom of a reduced operator evaluation $\left(\mathcal{L}_{\text{red}}\left[s_{\text{red}}^{k+1}, \mathbf{u}^{k+1}, \psi^{k+1}\right]\right)_n$ is defined as

$$\frac{1}{\Delta t}\left(a_n^{k+1} - a_n^k\right) - \sum_{m=1}^{M_s} \mathcal{L}_h[s_{\text{red}}^{k+1}, \psi_{\text{red}}^{k+1}](x_m^s) \underbrace{\int_\Omega \xi_m^s \varphi_n^s}_{(I)} - \underbrace{\int_\Omega q_1 \varphi_n^s}_{(II)} \quad (21)$$

for $n = 1,\ldots,N_s$,

$$\sum_{m=1}^{M_{\mathbf{u}}} \mathcal{L}_{\text{red}}\left[s_{\text{red}}^{k+1}, \psi_{\text{red}}^{k+1}\right](x_m^{\mathbf{u}}) \underbrace{\int_\Omega \xi_m^{\mathbf{u}} \varphi_{\hat{n}}^{\mathbf{u}}}_{(III)} - b_{\hat{n}}^{k+1} \quad (22)$$

for $n = N_s+1,\ldots,N_s+N_{\mathbf{u}}$ with $\hat{n} := n - N_s$,

$$\sum_{i=1}^{N_u} b_i^{k+1} \underbrace{\langle \varphi_i^{\mathbf{u}}, [\varphi_n^{\psi}] \rangle_{\mathcal{W}_h^{\mathbf{u}}}}_{(IV)} - \underbrace{\int_\Omega (q_1+q_2)\varphi_n^{\psi}}_{(V)} \quad (23)$$

Table 1. Costs of offline matrix computations

(I)	(II)	(III)	(IV)	(V)
$\mathcal{O}(N_s M_s H)$	$\mathcal{O}(N_s H)$	$\mathcal{O}(M_{\mathbf{u}} N_{\mathbf{u}} H)$	$\mathcal{O}(N_{\mathbf{u}} N_\psi H)$	$\mathcal{O}(N_\psi H)$

for $n = N_s+N_{\mathbf{u}}+1, \dots, N_s+N_{\mathbf{u}}+N_\psi$ with $\hat{n} := n-N_s-N_{\mathbf{u}}$ and

$$\sum_{i=1}^{N_\psi} c_i^{k+1} \int_\Omega \varphi_i^\psi \tag{24}$$

for $n = N_s + N_{\mathbf{u}} + N_\psi + 1$. In equation (23), the jump operator $[\cdot] : \mathcal{W}_h^{\mathcal{T}} \to \mathcal{W}_h^{\mathcal{E}}, u_h \mapsto [u_h]$ defined by $[u_h]_{\sigma_{ij}} := u_{h,i} - u_{h,j}$ for all $\sigma_{ij} \in \mathcal{S}$ is used. It measures the jump of a finite volume function on the mesh edges.

The integrals $(I) - (V)$ can be pre–computed during the offline phase at the costs given in Table 4.1.

Then, a single reduced operator evaluation has complexity $\mathcal{O}(N_s M_s + N_{\mathbf{u}} M_{\mathbf{u}} + N_\psi N_{\mathbf{u}})$ which is assumed to be significantly more efficient than the detailed operator evaluation (14) of complexity $\mathcal{O}(H)$. The same computations can be conducted for the Jacobian matrix $\mathbf{D}\mathcal{L}_{\text{red}}$. The costs for the matrix assembly are the same, whereas the solution of the linear equation system conducted in each Newton step 13 with the Jacobian on the left hand side has complexity $\mathcal{O}((N_s + N_{\mathbf{u}} + N_\psi)^3)$. The costs in the high–dimensional scheme add up to $\mathcal{O}((H)^3)$ here, in case of Gaussian elimination or $\mathcal{O}(H N_{\text{iter}})$ for an iterative solver with a maximum number of iterations N_{iter}.

5. EXPERIMENTS

In our experiments with the reduced basis method for the two–phase flow problem (1)-(3), we use similar data functions like in Michel (2004):

$$k_w(s) = \frac{s^3}{12}, \qquad k_{nw}(s) = \frac{(1-s)^3}{3},$$
$$M(s) = k_w(s) + k_{nw}(s), \qquad f(s) = \frac{k_w(s)}{M(s)} \text{ and}$$
$$p_c(s) = -0.5\sqrt{\frac{1-s}{s}}.$$

The source and sink terms (5) are given as characteristic functions on circles $B(\hat{x}, r) := \{x \in \mathbb{R}^2 | \, \|x - \hat{x}\| \le r\}$ by

$$\overline{q} = 10\ \mathbf{1}_{B((0.5,0.8),0.01)} + 20\ \mathbf{1}_{B((0.2,0.2),0.01)}$$
$$\underline{q} = 30\ \mathbf{1}_{B((0.8,0.5),0.01)}$$

and the injection constant $c = 0.8$. The initial saturation is set to 0.5 on the entire domain $\Omega := [0,1]^2$. The final time T is set to 0.5.

Discretization For the finite volume discretization a rectangular mesh with 400 control volumes and a time step length of $\Delta t = 0.01$ is used. Solution snapshots reconstructed from reduced simulations of the three unknowns at $t = 0.25$ and $t = 0.5$ are depicted in Figure 1.

Reduced basis method After computing the trajectory of solution snapshots with the scheme described in Definition 2.1, a POD is applied to compute the three reduced bases $\Phi^s, \Phi^{\mathbf{u}}$ and Φ^ψ. Discarding all POD modes with eigenvectors less than 10^{-6}, the resulting basis sizes are $N_s = 28$, $N_{\mathbf{u}} = 72$ and $N_\psi = 34$.

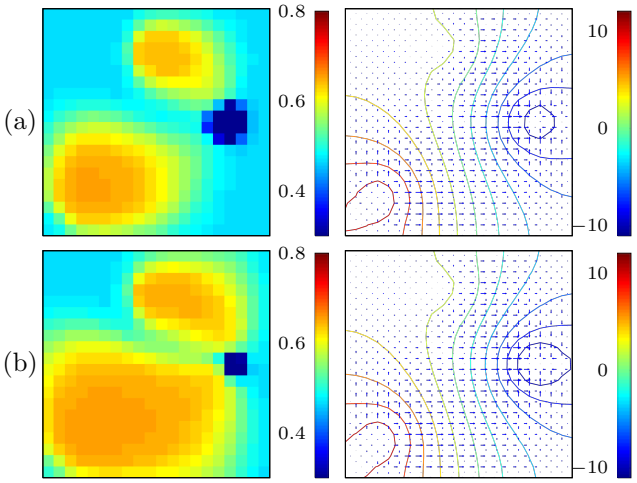

Fig. 1. Illustration of saturation concentration, and contour plot of pressure field with velocity flux at time instances (a) $t = 0.25$ and (b) $t = 0.5$. The snapshots are reconstructed from a reduced simulation.

Table 2. Error and timings of reduced simulations with different basis sizes.

$(N_s, N_{\mathbf{u}}, N_\psi)$	$(M_s, M_{\mathbf{u}})$	$\|s_h - s_{\text{red}}\|$	$\|\psi_h - \psi_{\text{red}}\|$	time
(28,72,34)	(387,386)	$6.2 \cdot 10^{-5}$	$4.11 \cdot 10^{-4}$	30.15
(28,72,34)	(75,75)	$1.03 \cdot 10^{-4}$	$2.11 \cdot 10^{-3}$	21.56
(28,72,34)	(75,125)	$7.59 \cdot 10^{-5}$	$8.69 \cdot 10^{-4}$	20.61
(23,58,28)	(75,125)	$2.47 \cdot 10^{-4}$	$2.55 \cdot 10^{-3}$	18.24

The empirical interpolation basis and interpolation points for the non–linear operators $\mathcal{L}_h^s$ and $\mathcal{L}_h^{\mathbf{u}}$ are derived with the EI-GREEDY algorithm for $\varepsilon_{\text{tol}} = 10^{-8}$ resulting in basis sizes $M_s = 387$ and $M_{\mathbf{u}} = 386$. The error convergence and the selected interpolation points are illustrated in Figures 2+3. We observe that the EI-GREEDY chooses the DOFs at different grid cells for the two operators resulting in two substantially different subgrids. Table 2 illustrates the reduced simulation computation time and the $L^2(\Omega)$ error between high dimensional and reduced discrete solutions for saturation and pressure. As the computation time of a high dimensional simulation is about 52 seconds, the computational gain is about 2.5. We observe that the empirical interpolation basis is oversized, as a reduced simulation with basis sizes $(M_s, M_{\mathbf{u}}) = (75, 125)$ achieves similarly good results as with all basis vectors.

6. CONCLUSION AND FURTHER WORK

This article shows the applicability of the reduced basis framework as introduced in Drohmann et al. (2010) to a non–linear system of PDEs modelling two–phase flow in a porous medium. Reduced basis spaces are generated independently for the three physical variables in this scheme and the two identified non–linear operators.

So far, the computations conducted for this presentation must be labelled as "toy sized" and we did not consider a parametrization of the problem. Therefor, an increase of size in spatial and parameter domain are the canonical steps to address in the future. This requires the development of efficient a posteriori error estimators and the use of more sophisticated algorithms to construct the reduced

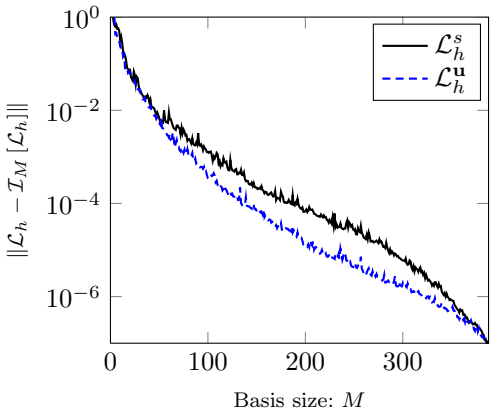

Fig. 2. Illustration of error convergence of EI-GREEDY algorithm for operators $\mathcal{L}_h^s$ and $\mathcal{L}_h^{\mathbf{u}}$.

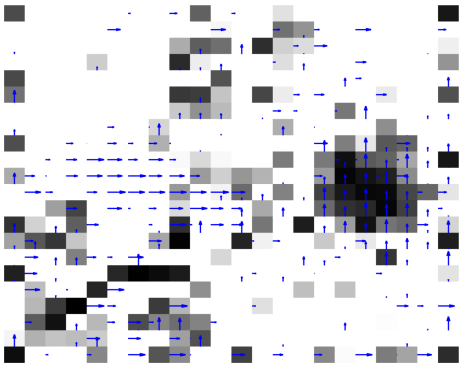

Fig. 3. Illustration of selected interpolation DOFs for operators $\mathcal{L}_h^s$ (control volumes) and $\mathcal{L}_h^{\mathbf{u}}$ (fluxes over edges). Darker shades of marked control volumes and longer arrows represent earlier selected DOFs.

basis spaces for the three physical variables like the POD-GREEDY or the PODEI-GREEDY algorithm in Drohmann et al. (2010) or adaptive reduced basis construction approaches as in Haasdonk et al. (2011) and Eftang et al. (2011). In this context, it is also worthwhile to study the effects of the Babuska–Brezzi condition on the stability of the pressure and velocity equations like it was done, e.g. in Rozza and Veroy (2007).

REFERENCES

Barrault, M., Maday, Y., Nguyen, N., and Patera, A. (2004). An 'empirical interpolation' method: application to efficient reduced-basis discretization of partial differential equations. *C. R. Math. Acad. Sci. Paris Series I*, 339, 667–672.

Carlberg, K., Bou-Mosleh, C., and Farhat, C. (2011). Efficient non-linear model reduction via a least-squares Petrov–Galerkin projection and compressive tensor approximations. *International Journal for Numerical Methods in Engineering*, 86(2), 155–181. doi: 10.1002/nme.3050.

Chaturantabut, S. and Sorensen, D.C. (2011). Application of POD and DEIM to dimension reduction of nonlinear miscible viscous fingering in porous media. *Math. Comput. Model. Dyn. Syst.*

Ciarlet, P. (1978). *The finite element method for elliptic problems*. North-Holland.

Drohmann, M., Haasdonk, B., and Ohlberger, M. (2010). Reduced basis approximation for nonlinear parametrized evolution equations based on empirical operator interpolation. Technical report, FB10, University of Münster.

Eftang, J.L., Knezevic, D.J., and Patera, A.T. (2011). An hp certified reduced basis method for parametrized parabolic partial differential equations. *Mathematical and Computer Modelling of Dynamical Systems*, 17(4), 395–422. doi:10.1080/13873954.2011.547670.

Grepl, M., Maday, Y., Nguyen, N., and Patera, A. (2007). Efficient reduced-basis treatment of nonaffine and nonlinear partial differential equations. *M2AN, Math. Model. Numer. Anal.*, 41(3), 575–605.

Haasdonk, B., Dihlmann, M., and Ohlberger, M. (2011). A training set and multiple bases generation approach for parametrized model reduction based on adaptive grids in parameter space. *Mathematical and Computer Modelling of Dynamical Systems*, 17(4), 423–442.

Haasdonk, B. and Ohlberger, M. (2008). Adaptive basis enrichment for the reduced basis method applied to finite volume schemes. In *Proc. 5th International Symposium on Finite Volumes for Complex Applications*, 471–478.

Haasdonk, B., Ohlberger, M., and Rozza, G. (2007). A reduced basis method for evolution schemes with parameter-dependent explicit operators. Technical Report 09/07 - N, FB 10, University of Münster. Accepted by ETNA.

Michel, A. (2004). A finite volume scheme for two-phase immiscible flow in porous media. *SIAM Journal on Numerical Analysis*, 41(4), 1301–1317.

Patera, A. and Rozza, G. (2007). *Reduced Basis Approximation and a Posteriori Error Estimation for Parametrized Partial Differential Equations*. MIT. Version 1.0, Copyright MIT 2006-2007, to appear in (tentative rubric) MIT Pappalardo Graduate Monographs in Mechanical Engineering.

Rozza, G. and Veroy, K. (2007). On the stability of the reduced basis method for stokes equations in parametrized domains. *Computer Methods in Applied Mechanics and Engineering*, 196(7), 1244 – 1260. doi: 10.1016/j.cma.2006.09.005.